treatment, $P = 0.029$; $F(16,152) = 5.894$ for treatment × time, $P = 0.0001$]. There were no significant differences between the initial EPSPs or EPSPs 30 min after injection in the three groups shown in Fig. 1C.

15. BAPTA was injected by diffusion or iontophoresis (0.5 to 1 nA, 500 ms at 1 Hz). Similar results were obtained after 20 to 30 min of iontophoretic injection or diffusion. BAPTA injected by these methods into the sensory neuron blocked synaptic transmission, suggesting that it was effective in buffering the Ca^{2+} concentration. In the experiments shown in Fig. 2, A and B, there were significant differences between homosynaptic depression (control), PTP, and PTP/BAPTA [for LFS synapses: $F(2,18) = 6.281$ for treatment, $P = 0.0085$; $F(16,144) = 2.428$ for treatment × time, $P = 0.0029$; for L7 synapses: $F(2,18) = 6.214$ for treatment, $P = 0.0089$; $F(16,144) = 7.191$ for treatment × time, $P = 0.0001$]. For LFS synapses, the average amplitudes of the EPSPs on trial one, 30 min after impalement, were 26.4 ± 4.4 mV (control), 23.3 ± 3.7 mV (PTP), and 20.9 ± 3.3 mV (PTP/BAPTA); for L7 synapses, they were 17.3 ± 3.1 mV, 12.6 ± 3.2 mV, and 16.9 ± 3.9 mV, respectively. There were no significant differences among EPSP amplitudes on trial one for the three groups at either synapse.
16. We manually applied 10 μl of 5-HT (50 μM) with a 50-μl Hamilton syringe to the vicinity of the cells, as previously described (2). Fast green (0.2%), which by itself did not affect synaptic transmission, was included in the 5-HT solution to check the delivery and location of the puff. The solution was washed out in less than 60 s by continuous perfusion of the culture. A two-way ANOVA revealed that 5-HT produced significant facilitation of EPSPs [overall, $F(2,13) = 8.852$ for treatment, $P = 0.0037$ and $F(16,104) = 5.718$ for treatment × time, $P = 0.0001$], but there was no significant difference between the 5-HT and 5-HT/BAPTA groups. The average amplitudes of EPSPs 30 min after impalement were 25.3 ± 5.1 mV (control) and 19.3 ± 4.6 mV (BAPTA) in the experiments shown in Fig. 3B, and 22.7 ± 6.4 mV (control), 28.8 ± 3.6 mV (5-HT), and 20.1 ± 4.2 mV (5-HT/BAPTA) in the experiments shown in Fig. 3C. There were no significant differences among EPSP amplitudes on trial one for the different groups.
17. V. F. Castellucci and E. R. Kandel, *Proc. Natl. Acad. Sci. U.S.A.* **71**, 5004 (1974).
18. N. Dale and E. R. Kandel, *J. Physiol. (London)* **421**, 203 (1990).
19. LFS motor neurons were injected with 2 nA of current and L7 motor neurons with 4 nA, which produced approximately 50 to 100 mV of additional hyperpolarization below the level at which the motor neurons were held throughout the rest of the experiment (*8*), as measured in the soma. However, the hyperpolarization could have been substantially less at the synaptic region. Overall, there were significant differences between control, PTP, and PTP with hyperpolarization during the tetanus (PTP/HPP) [for LFS synapses: $F(2,14) = 6.771$ for treatment, $P = 0.0088$; $F(16,112) = 4.807$ for treatment × time, $P = 0.0001$; for L7 synapses: $F(2,19) = 5.22$ for treatment, $P = 0.0156$; $F(16,152) = 2.951$ for treatment × time, $P = 0.0003$]. For LFS synapses, EPSPs 30 min after impalement had amplitudes of 18.3 ± 2.5 mV (control), 21.3 ± 5.1 mV (PTP), and 22.1 ± 3.8 mV (PTP/HPP); for L7 synapses, they were 14.6 ± 2.6 mV, 19.5 ± 4.0 mV, and 18.1 ± 3.2 mV, respectively. There were no significant differences among EPSP amplitudes on trial one for these three groups.
20. Electrical coupling between the sensory neuron and motor neuron was monitored by impaling both cells with microelectrodes and applying a hyperpolarizing pulse (30 to 120 mV) to one cell (cell 1) and measuring the change of membrane potential in the other (cell 2). The degree of coupling was defined by: (membrane potential change in cell 2/hyperpolarizing potential applied in cell 1) × 100%. The coupling measured from soma to soma was 1.02 ± 0.49% ($n = 5$) from sensory to LFS cell, 0.79 ± 0.38% ($n = 5$) from LFS to sensory cell, 0.32 ± 0.17% ($n = 8$) from sensory to L7 cell, and 0.23 ± 0.12% ($n = 8$) from L7 to sensory cell.
21. M. V. L. Bennett *et al. Neuron* **6**, 305 (1991); R. Yuste, D. A. Nelson, W. W. Rubin, L. C. Katz, *ibid.* **14**, 7 (1995).
22. Overall, there were significant differences between control, PTP in the presence of octanol (PTP/octanol), and PTP with hyperpolarization during the tetanus in the presence of octanol [(PTP/HPP)/octanol] [$F(2,15) = 10.068$ for treatment, $P = 0.0176$ and $F(16,132) = 4.594$ for treatment × time, $P = 0.0001$]. EPSPs 30 min after impalement had amplitudes of 14.9 ± 2.3 mV (control), 11.6 ± 1.5 mV (PTP/octanol), and 12.0 ± 4.1 mV [(PTP/HPP)/octanol]. There were no significant differences among EPSP amplitudes on trial one for these three groups.
23. Recording of spontaneous mEPSPs was made at high gain, filtered at 300 Hz (−3 dB), and AC coupled. In experiments in which both evoked and spontaneous mEPSPs were measured, eEPSPs were recorded at low gain and DC coupled. Signals were digitized off-line with a PC-based ""fetchex" program (part of the ""pclamp" package, Axon Instruments) and analyzed with an ""axobasic" program. We visually identified mEPSPs on the basis of the following criteria: (i) a rise time of 3 to 20 ms, (ii) a half-decay time of at least 5 ms, and (iii) a minimum amplitude of 50 μV, which was usually about 25% greater than the peak-to-peak noise level (*3 18*). The frequency and the peak amplitude of mEPSPs were then automatically determined by the computer. When the dependent variable was the amplitude of eEPSPs (Fig. 4A), There were significant differences between the PTP and PTP/HPP groups [$F(1,10) = 5.244$ for treatment, $P = 0.045$ and $F(8,80) = 6.189$ for treatment × time, $P = 0.001$). EPSPs 30 min after impalement had amplitudes of 17.8 ± 2.9 mV (PTP) and 25.9 ± 2.3 mV (PTP/HPP) (not significantly different). When the dependent variable was the frequency of mEPSPs (Fig. 4B), there were no significant differences between PTP and PTP/HPP groups. The average frequency of mEPSPs 30 min after impalement was 0.032 ± 0.006 Hz and 0.041 ± 0.007 Hz for PTP and PTP/HPP groups, respectively (not significantly different).
24. A. R. Martin and G. Pilar, *J. Physiol. (London)* **175**, 17 (1964); H. P. Clamann, J. Mathis, H. R. Luscher, *J. Neurophysiol.* **61**, 403 (1989); W. H. Griffith, *ibid.* **63**, 491 (1990).
25. R. Anwyl, D. Mulkeen, M. J. Rowan, *Brain Res.* **503**, 148 (1989); R. C. Malenka, *Neuron* **6**, 53 (1991).
26. T. J. O'Dell, R. D. Hawkins, E. R. Kandel, O. Arancio, *Proc. Natl. Acad. Sci. U.S.A.* **88**, 11285 (1991); M. Zhuo, S. A. Small, E. R. Kandel, R. D. Hawkins, *Science* **260**, 1946 (1993).
27. R. K. Murphey and G. W. Davis, *J. Neurobiol.* **25**, 595 (1994); Y.-J. Lo, Y.-C. Lin, D. H. Sanes, M.-M. Poo, *J. Neurosci.* **14**, 4694 (1994).
28. Supported by grants from the National Institute of Mental Health (MH 26212) and the Howard Hughes Medical Institute. A long-term fellowship from the Human Frontier Science Program Organization to J.-X.B. is gratefully acknowledged.

15 July 1996; accepted 14 November 1996

A Mammalian Telomerase-Associated Protein

Lea Harrington,* Timothy McPhail, Vernon Mar, Wen Zhou, Rena Oulton, Amgen EST Program, Mike B. Bass, Isabel Arruda, Murray O. Robinson*

The telomerase ribonucleoprotein catalyzes the addition of new telomeres onto chromosome ends. A gene encoding a mammalian telomerase homolog called TP1 (telomerase-associated protein 1) was identified and cloned. TP1 exhibited extensive amino acid similarity to the *Tetrahymena* telomerase protein p80 and was shown to interact specifically with mammalian telomerase RNA. Antiserum to TP1 immunoprecipitated telomerase activity from cell extracts, suggesting that TP1 is associated with telomerase in vivo. The identification of TP1 suggests that telomerase-associated proteins are conserved from ciliates to humans.

Telomerase is an unusual RNA-dependent DNA polymerase that uses an RNA component to specify the addition of telomeric repeat sequences to chromosome ends (*1*). In humans the telomeric repeat is 5′-TTAGGG-3′, and the telomerase RNA contains a sequence complementary to this telomeric repeat (*2, 3*). The telomerase RNA template is required for telomere repeat synthesis in vitro and in vivo (*4–6*). Telomerase activity is differentially regulated in normal and immortalized cells. In germline cells telomeres are maintained, whereas several somatic tissues lack telomerase activity and undergo progressive telomere shortening with increasing age (*1*). In immortalized cells telomere length is stabilized and telomerase activity is often reactivated (*7–9*). Telomerase activity has also been detected in many cancers (*1, 9*).

Telomerase activities have been identified in several organisms, and their RNA components have been cloned from mouse, human, yeast, and several ciliates (*1*). Putative telomerase or telomere-associated proteins have been identified in yeast (*10*). The ribonucleoprotein complex responsible for telomerase activity, however, has been purified only in ciliates (*11–13*). Purified *Tetrahymena* telomerase contains an RNA and two protein components, p80 and p95 (*4, 13*). The p80 component can be specifically cross-linked to

L. Harrington, R. Oulton, I. Arruda, Ontario Cancer Institute–Amgen Institute, Department of Medical Biophysics, University of Toronto, 620 University Avenue, Toronto, Ontario M5G 2C1, Canada.
T. McPhail, V. Mar, W. Zhou, Amgen EST Program, M. B. Bass, M. O. Robinson, Amgen, Inc., 1840 DeHavilland Drive, Thousand Oaks, CA 91320, USA.

*To whom correspondence should be addressed.

telomerase RNA, whereas the p95 component binds and cross-links to single-stranded, telomeric DNA (*11, 13*). Antiserum to *Tetrahymena* p80 is also able to specifically immunoprecipitate telomerase activity from *Tetrahymena* cell extracts (*13*).

A cDNA encoding a *Tetrahymena* p80 homolog was identified from a murine colonic crypt expressed sequence tag (EST) database. Overlapping clones were subsequently identified from both a colonic crypt library and a bone marrow stromal cell library. The resultant contiguous cDNA sequence was 8160 nucleotides long and contained a single open reading frame (ORF) of 2629 amino acids. On the basis of functional criteria described below, the sequence was termed telomerase-associated protein 1 (TP1). The mouse sequence was used as a probe to identify contiguous human cDNA clones from a library prepared from a human colon carcinoma LIM1863 cell line. The mouse and human ORFs are 75% identical at the amino acid level (Fig. 1).

Three regions in the NH_2-terminal one-third of TP1 exhibited amino acid similarity to *Tetrahymena* p80 (Fig. 1, A and B). Region 2 showed the most homology to p80 with 46% identity over 90 amino acids (Fig. 1B). Other common motifs were also identified in the mouse and human TP1 protein. A Procite search identified an adenosine triphosphate/guanosine triphosphate (ATP/GTP) binding motif, beginning at amino acid 1179 of the mouse sequence (Fig. 1B). A 30–amino acid repeated sequence at the NH_2-terminus of TP1 (R1 to R4) showed weak homology to a protein of unknown function in the ononis yellow mosaic tymovirus (*14*) (Fig. 1A). The COOH-terminal third of TP1 contained 16 putative WD40 repeats (Fig. 1A) (*15*).

To determine the tissue distribution of the *TP1* transcripts, we performed Northern (RNA) blot analysis on RNAs from adult mouse tissues. An ~8–kilobase pair (kbp) transcript was detected at varying levels in multiple tissues with a murine *TP1* RNA probe (Fig. 2A). Human tissues also showed widespread expression of *TP1* mRNA and often contained two transcripts of 8 and 9.5 kbp (Fig. 2B). Expression of *TP1* mRNA was also observed in all human and murine cell lines examined, including nontransformed primary cells such as human fore-

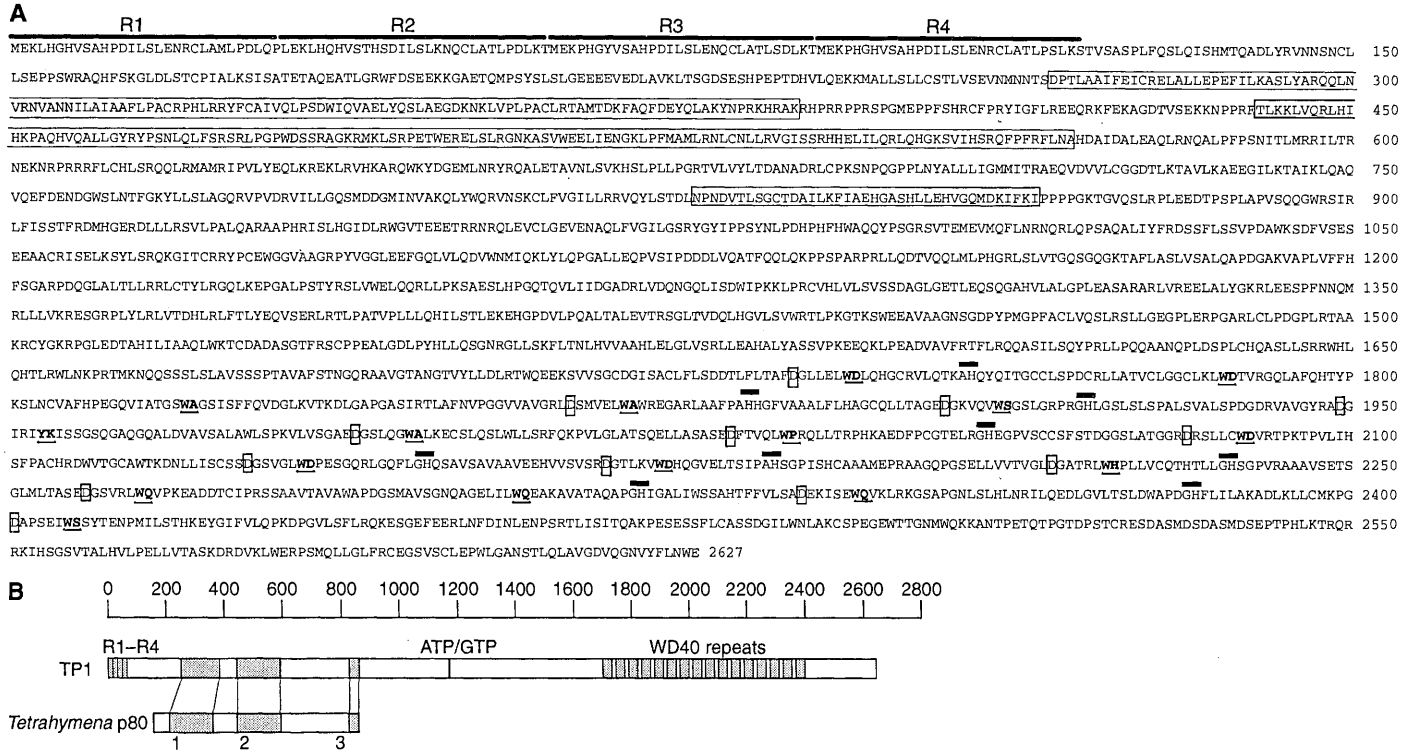

Fig. 1. (**A**) Amino acid sequence of human TP1. Four NH_2-terminal repeats of unknown significance are indicated by solid lines over the sequence (R1 to R4). Boxed regions show homology to *Tetrahymena* p80. Amino acids corresponding to the WD40 consensus sequence of the putative WD40 repeats are indicated as follows: Conserved "WD motif" amino acid pairs are in boldface and underlined; conserved D residues are boxed; conserved "GH motif" residues are overlined. Abbreviations for the amino acid residues are as follows: A, Ala; C, Cys; D, Asp; E, Glu; F, Phe; G, Gly; H, His; I, Ile; K, Lys; L, Leu; M, Met; N, Asn; P, Pro; Q, Gln; R, Arg; S, Ser; T, Thr; V, Val; W, Trp; and Y, Tyr. The complete human and murine TP1 sequences have been deposited with GenBank (accession numbers U86136 and U86137, respectively). (**B**) (Top) The TP1 amino acid sequence is depicted schematically, with boxed regions as follows: NH_2-terminal repeats 1 to 4 (R1–R4); gray boxes (1 to 3) show regions of homology between TP1 and *Tetrahymena* p80; and 16 putative WD40 repeats are boxed. (Bottom) Human (Hu) and murine (Mu) TP1 amino acid sequences were aligned to *Tetrahymena* p80 by means of a PAM250 matrix and then adjusted manually; *Tetrahymena* (Te) sequences identical to either human or mouse at each position are shown in boldface. The underlined, 90–amino acid segment in region 2 contains 46% identity between p80 and human TP1. Seventy amino acids of human TP1 (amino acids 484 to 554) also show 18% identity to the human Ro/SS ribonucleoprotein (the corresponding p80 sequence shows 29% identity) (*31*).

skin fibroblasts (*16*).

To determine whether TP1 interacts with telomerase RNA, we used a three-hybrid screen, a version of the two-hybrid screen in which an RNA fusion to the hairpin sequence of phage MS2 is used to activate transcription through an interaction with the MS2 coat protein (*17*). The NH_2-terminus of murine TP1, which contained the region with *Tetrahymena* p80 homology, was tested for interaction with mouse telomerase RNA (mTR) (Fig. 3). Coexpression of TP1 and mTR resulted in strong activation of the reporter genes *HIS3* and *lacZ* and allowed growth on 3-aminotriazole (3-AT) medium and detection of β-galactosidase (β-Gal) activity (Fig. 3, A and B). TP1 also interacted with a mutant mTR, mTR-1, but not with several control RNAs such as yeast U2, U4, and U6 small nuclear RNAs (snRNAs), the yeast telomerase RNA *TLC1*, and antisense mTR ("RTm") (Fig. 3, A and B). Another negative control, in which the MS2 tag was placed in an antisense direction relative to mTR ("2SM"), also did not allow growth on 3-AT medium (Fig. 3). Coexpression of TP1 and the iron response element, IRE, resulted in growth on 3-AT medium (*18*); however, β-Gal expression was not significantly above background levels (Fig. 3B). Only mTR and TP1 together resulted in the strong activation of both reporter genes in the three-hybrid assay, suggesting that TP1 is not a general RNA binding protein, but specifically binds telomerase RNA.

To determine whether TP1 associated with telomerase RNA and telomerase activity in vivo, we transfected a murine TP1 cDNA containing two copies of an NH_2- terminal Myc-epitope tag into murine neuroblastoma (N2A) cells. We then examined the cell lysates for immunoprecipitation of TP1 and telomerase activity using a monoclonal antibody to the Myc epitope (anti-Myc) (Fig. 4, A and B). Immunoblot analysis of the immunoprecipitates with anti-Myc confirmed that tagged TP1 was expressed in the transfected N2A cells (Fig. 4A). Telomerase activity was immunoprecipitated from Myc-TP1–transfected cells, but not from mock-transfected lysates, or Myc-TP1 lysates incubated with excess Myc peptide (Fig. 4B). Addition of a nonspecific peptide did not compete for the ability of anti-Myc to immunoprecipitate TP1 and telomerase activity (Fig. 4A, lane 6, and Fig. 4B, lane 11). We also examined whether anti-peptide antibodies against murine TP1 could immunoprecipitate telomerase activity from untransfected, immortalized mouse fibroblast (NIH 3T3) cell lysates (Fig. 4C). Telomerase activity was immunoprecipitated with an antipeptide antibody to the COOH-terminus of TP1 (Fig. 4C, lane 8) but was not immunoprecipitated by protein A resin alone or by preimmune serum (Fig. 4C, lanes 6 and 7). The immunoprecipitation of telomerase activity was specifically competed by incubation of the antipeptide antiserum with excess peptide to which the antibodies were raised (P3), but was not competed by another TP1 peptide, P1 (Fig. 4C, lanes 9 and 10). Reverse transcription and polymerase chain reaction (RT-PCR) analysis was used to establish that mTR was present when TP1, and telomerase activity, were immunoprecipitated (Fig. 4D).

These experiments demonstrate that TP1 interacts with telomerase RNA and that TP1 is associated with telomerase activity in vivo. Further biochemical analysis is required to determine whether TP1 is essential for telomerase function. The NH_2-terminus of TP1, which shows the most homology to *Tetrahymena* p80, is sufficient to bind telomerase RNA in vivo. These results support the suggestion that although the telomerase RNAs of ciliates and mammals differ considerably in sequence (*3*, *4*, *19*), they may share sufficient secondary structure to be recognized by a conserved RNA-binding motif (*20*).

The TP1 sequence has features distinct from that of p80. Unlike p80, TP1 does not contain a putative zinc finger (*13*). The significance of the potential ATP/GTP-binding domain is unknown, because ATP is apparently not required for human or mouse telomerase activity (*2*, *21*). An intriguing feature of the TP1 sequence is the WD40 repeats in the COOH-terminus. The β subunit of the heterotrimeric GTP-binding protein is composed of seven WD40 repeats that form a structure resembling a seven-bladed propeller (*22*). Similar WD40 repeats are present in a number of proteins that form multiprotein complexes (*15*). TP1 may form one or more propeller structures that mediate interactions with other telomerase or telomere-binding proteins, such as the telomeric

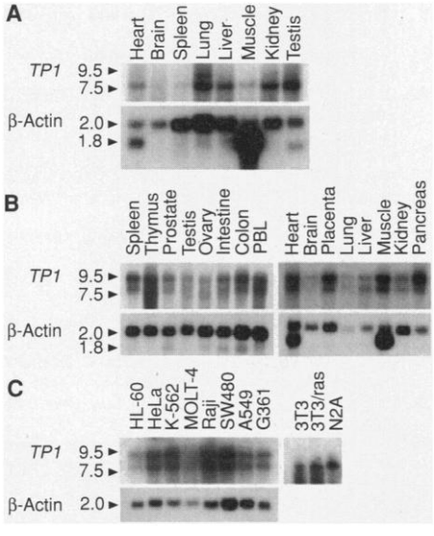

Fig. 2. Expression of murine and human *TP1* mRNA in tissues and cell lines. (**A**) Northern blots from the indicated murine tissues (Clontech, San Diego, California) were probed with ^{32}P-labeled murine *TP1* RNA probe (top) and with random-primed β-actin probe (bottom). (**B**) Northern blot of the indicated human RNA samples (Clontech), probed with human *TP1* RNA probe as in (A). (**C**) Northern blot of mRNA from immortalized human and mouse cell lines. (Left) RNA from the indicated immortalized human cell lines (Clontech) was probed with human *TP1* and β-actin as in (B); (right) RNA from the indicated murine cell lines was probed with murine *TP1* as in (A). Molecular sizes are indicated on the left (in kilobase pairs).

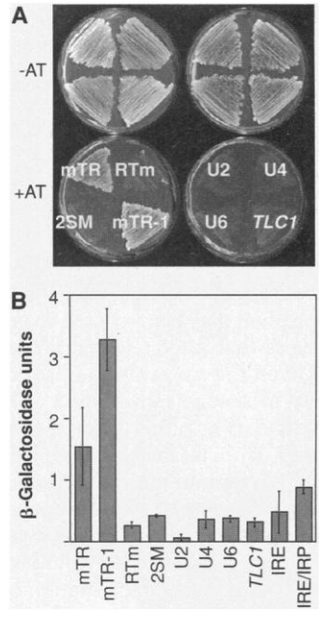

Fig. 3. Three-hybrid analysis of the mTP1 and mTR interaction. (**A**) Various MS2-tagged RNAs as indicated were cotransformed with TP1 into the three-hybrid yeast strain L40-coat and patched on synthetic drop-out plates lacking uracil and leucine (−AT) and the same plates also lacking histidine and containing 5 mM 3-aminotriazole (+AT) (*17*). An interaction between the tagged RNA and TP1 allows growth on 3-AT. mTR is wild-type mouse telomerase RNA (*19*); RTm indicates the mTR sequence cloned in the antisense direction relative to the MS2 hairpins; 2SM refers to the full-length mTR in the sense direction and the MS2 hairpins in the antisense direction; mTR-1 is a mutant containing three nucleotide substitutions: $C^{142}\rightarrow T$, $G^{202}\rightarrow C$, and $G^{227}\rightarrow A$ [relative to the transcription start site (*19*)]; U2, U4, and U6 are yeast snRNAs (U6 is not MS2-tagged) (*32*); and *TLC1* is the full-length yeast telomerase RNA (*16*). (**B**) β-Galactosidase assays on transformants shown in (A). Liquid β-Gal assays were performed in triplicate and quantified as in (*29*), with 10^{-3} standard β-Gal units (420 nm) shown on the *y* axis. Error bars indicate standard deviation for each sample average. Another control RNA, the iron response element hairpin IRE (*17*), is shown for comparison to mTR and mTR-1. Although cotransformation of TP1 and IRE resulted in growth on 3-AT medium, β-Gal levels were not significantly above those of other negative controls (*18*). A positive control for the three-hybrid interaction, consisting of IRE and its binding protein IRP (IRE/IRP) (*17*), is shown at right.

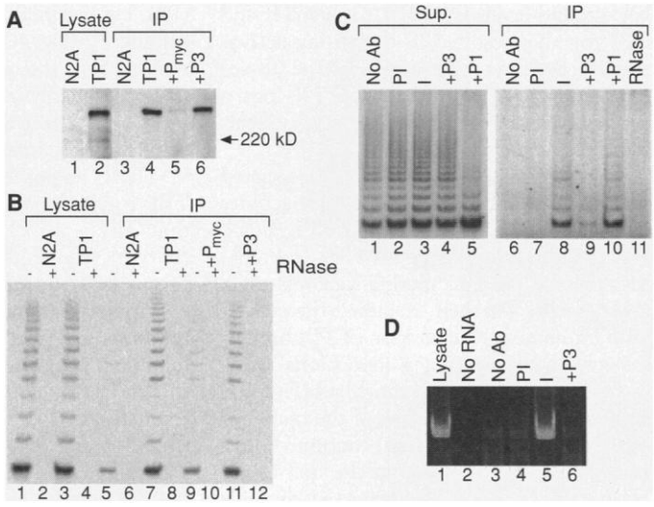

Fig. 4. Telomerase activity in TP1 immunoprecipitates. (**A**) Immunoblot developed with an antibody to Myc. S100 lysates (lanes 1 and 2) and immunoprecipitates (lanes 3 to 6) of N2A cells transfected with a Myc-epitope fusion gene containing the entire murine TP1 coding sequence (TP1; lanes 2, and 4 to 6) and mock-transfected cells (lanes 1 and 3) were resolved by SDS–polyacrylamide gel electrophoresis, transferred to nylon membrane, and probed with anti-Myc (*33*). The Myc-TP1 in the TP1 cell lysate and in the TP1 immunoprecipitate can be detected above the 220-kD protein marker indicated at right. Lanes 5 and 6: 10 μg of Myc peptide [sequence: 408-AEEQKLISEEDLLRKRREQLKHKLEQLRNSCA] (lane 5), or the non-specific peptide P3 (lane 6, see also below) were incubated with anti-Myc before the immunoprecipitation to demonstrate the antibody specificity. No TP1 degradation products were detected below the region shown. (**B**) Telomerase activity in cells transfected with Myc-TP1 and mock-transfected cells as in (A). Protein G beads were assayed for telomerase activity through use of the telomere repeat amplification protocol (TRAP) (*30*), in the absence (odd-numbered lanes) and presence (even-numbered lanes) of 5 μg of ribonuclease A (RNase) (Sigma). Lanes 9 and 11: Myc peptide and P3 peptide (10 μg each) were added as competitor to the immunoprecipitation of Myc-TP1 lysates in lane 7. (**C**) Immunoprecipitation of telomerase activity by antipeptide antibodies against murine TP1. DEAE-purified NIH 3T3 S100 cell lysates were precipitated onto protein A–Sepharose beads adsorbed with the following: no antibody (lanes 1 and 6); normal rabbit preimmune sera (lanes 2 and 7); rabbit antisera raised against a COOH-terminal TP1 peptide, P3 [sequence: 1536-DPDASGTFRSCPPEALKDL] (lanes 3 and 8); antibodies to P3 peptide in the presence of 60 μg of P3 peptide (lanes 4 and 9); and antibodies to P3 peptide plus 60 μg of an NH_2-terminal TP1 peptide, P1 [sequence: 390-RSKRRSRQPPRPQKTERPFSERGK] (lanes 5 and 10) (*33*). Both the supernatants after incubation with 3T3 S100 lysate (Sup; lanes 1 to 5) and the washed beads (IP; lanes 6 to 10) were assayed by TRAP and resolved on a 10% acrylamide nondenaturing gel. Lane 11: RNase treatment of the immunoprecipitate in lane 8. Similar results were obtained with both Myc-TP1–transfected N2A cell lysates and NIH 3T3 cell lysates ($n = 6$). (**D**) Analysis of mTR in the TP1 immunoprecipitates. Approximately 5 μl of protein A beads were phenol-extracted and subjected to RT-PCR with mTR-specific primers as in (*19*). Lanes 1 and 2: positive control lysate (NIH 3T3) and "no RNA" negative controls; lanes 3 to 6: no antibody, preimmune, immune, and immune plus P3 peptide [as in (C)].

repeat binding factor TRF (*23*).

The expression pattern of *TP1* mRNA was not restricted to tissues and cell lines that express telomerase activity, but showed varied expression levels in several tissues (*1*, *9*). Mouse and human telomerase RNAs are also expressed in multiple tissues (*1*, *3*, *19*, *24*). TP1 may not be a rate-limiting or essential subunit, or perhaps associated proteins inhibit telomerase activity in some cell types. Alternatively, TP1 protein expression may be restricted to only those cell types that have telomerase activity (*1*, *9*). Given the reactivation of telomerase activity in several transformed cells and tumor tissues (*9*), inhibitors of the association of TP1 with telomerase may yield useful reagents for inhibition of certain cancers. Our identification of TP1 suggests that telomerases between organisms as divergent as ciliates and humans are similar and should facilitate the characterization of other components of mammalian telomerase.

REFERENCES AND NOTES

1. C. W. Greider, *Annu. Rev. Biochem.* **65**, 337 (1996).
2. G. B. Morin, *Cell* **59**, 521 (1989).
3. J. Feng *et al.*, *Science* **269**, 1236 (1995).
4. C. W. Greider and E. H. Blackburn, *Nature* **337**, 331 (1989).
5. D. Shippen-Lentz and E. H. Blackburn, *Science* **247**, 546 (1990); G.-L. Yu, J. D. Bradley, L. D. Attardi, E. H. Blackburn, *Nature* **344**, 126 (1990); D. Gilley, M. S. Lee, E. H. Blackburn, *Genes Dev.* **9**, 2214 (1995); M. J. McEachern and E. H. Blackburn, *Nature* **376**, 403 (1995); C. Autexier and C. W. Greider, *Genes Dev.* **9**, 2227 (1995); C. Autexier, R. Pruzan, W. D. Funk, C. W. Greider, *EMBO J.* **15**, 5928 (1996).
6. M. S. Singer and D. E. Gottschling, *Science* **266**, 404 (1995).
7. C. M. Counter *et al.*, *EMBO J.* **11**, 1921 (1992).
8. T. M. Bryan, A. Englezou, J. Gupta, S. Bacchetti, R. R. Reddel, *ibid.* **14**, 4240 (1995).
9. C. Autexier and C. W. Greider, *Trends Biochem. Sci.* **21**, 387 (1996).
10. V. Lundblad and J. W. Szostak, *Cell* **57**, 633 (1989); C. I. Nugent, T. R. Hughes, N. F. Lue, V. Lundblad, *Science* **274**, 249 (1996); T. S. Lendvay, D. K. Morris, J. Sah, B. Balasubramanian, V. Lundblad, *Genetics* **144**, 1399 (1996).
11. L. Harrington, C. Hull, J. Crittenden, C. Greider, *J. Biol. Chem.* **270**, 8893 (1995).
12. J. Lingner and T. R. Cech, *Proc. Natl. Acad. Sci. U.S.A.* **93**, 10712 (1996).
13. K. Collins, R. Kobayashi, C. W. Greider, *Cell* **81**, 677 (1995).
14. S. W. Ding, P. Keese, A. Gibbs, *Virology* **172**, 555 (1989).
15. E. J. Neer, C. J. Schmidt, R. Nambudripad, T. F. Smith, *Nature* **371**, 297 (1994).
16. W. Zhou and M. O. Robinson, unpublished data.
17. D. J. Sengupta *et al.*, *Proc. Natl. Acad. Sci. U.S.A.* **93**, 8496 (1996). For testing the mTR-TP1 interaction in this screen, the full-length mouse telomerase RNA gene, mTR (*19*), was tagged at its 3′ end with two MS2 hairpins and inserted into the *RPR1* promoter-terminator of pIIIEx426 containing a *URA3*-selectable marker (*25*). The RNA molecules "RTm," "2SM," *TLC1*, and mTR-1 were constructed in a similar manner. Yeast U2 and U4 snRNAs were similarly tagged with the MS2 hairpins, U6 was not tagged, and all were inserted into the *URA3*-selectable plasmid, pRS316 (*26*). For the GAL4 activation domain (AD)–TP1 fusion protein, an Ssp I–Xba I fragment of plasmid pCR3MycTag2 (1 to 871 amino acids of murine TP1) was blunt-ended and cloned into Bam HI, blunt-ended pACTII containing a *LEU2*-selectable marker (*27*). The RNA and GAL4 fusion plasmids were transformed (*28*) into strain L40-coat, which carries an integrated copy of the MS2 coat protein fused to the lexA DNA binding domain. Cotransformants were selected by culturing the cells on yeast agar plates (SD) lacking leucine (−LEU) and uracil (−URA) at 30°C (*29*). Cotransformants were patched onto SD-URA-LEU plates, and SD-URA-LEU-HIS plates containing 5 to 20 mM 3-AT (Sigma), and incubated for 3 days at 30°C. Liquid β-Gal assays were performed as in (*29*).
18. I. Arruda and L. Harrington, unpublished data.
19. M. A. Blasco, W. Funk, B. Villeponteau, C. W. Greider, *Science* **269**, 1267 (1995).
20. D. P. Romero and E. H. Blackburn, *Cell* **67**, 343 (1991); E. ten-Dam, A. van-Belkum, K. Pleij, *Nucleic Acids Res.* **19**, 6951 (1991); J. Lingner, L. L. Hendrick, T. R. Cech, *Genes Dev.* **8**, 1984 (1994); M. McCormick-Graham and D. P. Romero, *Nucleic Acids Res.* **23**, 1091 (1995); A. J. Zaug and T. R. Cech, *RNA* **1**, 363 (1995).
21. K. R. Prowse, A. A. Avilion, C. W. Greider, *Proc. Natl. Acad. Sci. U.S.A.* **90**, 1493 (1993).
22. D. G. Lambright *et al.*, *Nature* **379**, 311 (1996); J. Sondek, A. Bohm, D. G. Lambright, H. E. Hamm, P. B. Sigler, *ibid.*, p. 369.
23. L. Chong *et al.*, *Science* **270**, 1663 (1995).
24. A. A. Avilion *et al.*, *Cancer Res.* **56**, 645 (1996); M. A. Blasco, M. Rizen, C. W. Greider, D. Hanahan, *Nature Genet.* **2**, 200 (1996).
25. P. D. Good and D. R. Engelke, *Gene* **151**, 209 (1994).
26. R. S. Sikorski and P. A. Hieter, *Genetics* **122**, 19 (1989).
27. T. Durfee *et al.*, *Genes Dev.* **7**, 555 (1993); J. W. Harper, G. R. Adami, N. Wei, K. Keyomarsi, S. J. Elledge, *Cell* **75**, (1993); P. Legrain, M.-C. Dokhelar, C. Transy, *Nucleic Acids Res.* **22**, 3241 (1994).
28. D.-C. Chen, B.-C. Yang, T.-T. Kuo, *Curr. Genet.* **21**, 83 (1992).
29. C. Kaiser, S. Michaelis, A. Mitchell, *Methods in Yeast Genetics* (Cold Spring Harbor Laboratory Press, Cold Spring Harbor, NY, 1994).
30. N. Kim *et al.*, *Science* **266**, 2011 (1994).
31. S. L. Deutscher, J. B. Harley, J. D. Keene, *Proc. Natl. Acad. Sci. U.S.A.* **85**, 9479 (1988).
32. D. Tollervey, J. A. Wise, C. Guthrie, *Cell* **35**, 753 (1983); D. A. Brow and C. Guthrie, *Nature* **334**, 213 (1988); M. Ares, *Cell* **47**, 49 (1986).
33. At 24 hours before transfection, mouse neuroblastoma (N2A) cells were seeded at 7×10^5 cells per 100-mm dish in 15 ml of Dulbecco's modified Eagle's medium plus 10% (v/v) fetal calf serum (FCS). For the lipofection, cells were incubated in 6 ml of Optimem I reduced serum medium (Gibco-BRL), 174 μg of Pfx-6 (Invitrogen, San Diego, CA), and 29 μg of full-length, tagged TP1 plasmid DNA (PCR3Myctag3) for 4 hours. The medium was replaced with fresh media containing 10% (v/v) FCS, and the cells were harvested 24 hours later as in (*7*). Protein lysates were subjected to electrophoresis on 6% (w/v) SDS–polyacrylamide gels and transferred to a nylon membrane. The membrane was incubated with an antibody to Myc (Oncogene Science, San Di-

ego, CA) followed by a horseradish peroxidase–conjugated secondary antibody (Amersham, Arlington Heights, IL) and visualized with the use of an Amersham ECL kit (Amersham). Diethylaminoethyl (DEAE) agarose (Bio-Rad, Hercules, CA) column chromatography was performed as in (*21*). Approximately 0.5 μg of antibody to human Myc (Oncogene Science) was incubated with 100 to 200 μg of N2A S100 lysate from cells expressing either the Myc-tagged, full-length TP1 (TP1), or with no plasmid (N2A), for 1 hour, followed by incubation with 5 to 10 μl of protein G–Sepharose beads at 4°C for 1 to 3 hours. For the Myc peptide competition, 10 μg of Myc peptide (Oncogene Science) was added before incubation with anti-Myc. The supernatant was removed, and the beads were washed twice with 1 ml of 2.3× hypobuffer (*7*) containing 10% (v/v) glycerol and 0.1 M NaCl. The lysates (lysate) and immunoprecipitates (IP) were assayed by the telomerase repeat amplification protocol (TRAP) (*30*). For the anti-peptide immunoprecipitations, sera was adsorbed to 10 μl of protein A–Sepharose beads (Pierce, Rockford, IL), washed with hypobuffer, and incubated with DEAE-purified S100 lysates of NIH 3T3 cells. For peptide competition, 60 μg of each peptide was incubated with the washed protein A beads before the addition of lysate.

34. We thank D. Yeung, L. Antonio, A. Kroll, M. Rihanek, T. Zamborelli A. Hessel, D. Field, J. Hu, and J. Friesen for reagents and technical help; T. Mak, D. Bentley, S. Benchimol, and M. Tyers for helpful discussions and critical reading of the manuscript; and D. Sengupta, M. Wickens, and S. Fields for sharing three-hybrid reagents before publication. The Amgen EST Program is a large interdisciplinary group, who collectively made significant contributions to this work.

27 November 1996; accepted 21 January 1997

Immunoglobulin E Production in the Absence of Interleukin-4–Secreting CD1-Dependent Cells

Stephen T. Smiley, Mark H. Kaplan, Michael J. Grusby*

A lymphocyte population that expresses surface markers found on T cells and natural killer (NK) cells secretes large amounts of interleukin-4 (IL-4) immediately after T cell receptor ligation. These NK-like T cells are thus thought to be important for the initiation of type 2 T helper cell (T_H2) responses. CD1-deficient mice were found to lack this lymphocyte subset, but they could nevertheless mount a protypical T_H2 response; after immunization with antibody to immunoglobulin D (IgD), CD1-deficient mice produced IgE. Thus, although dependent on CD1 for their development, IL-4–secreting NK-like T cells are not required for T_H2 responses.

Interleukin-4 is critical for the differentiation of naïve T cells into T_H2 cells. Perhaps the most compelling evidence for this are studies showing that knockout mice harboring gene disruptions for either IL-4 (*1*) or STAT6, the signaling molecule activated by IL-4 (*2*, *3*), fail to generate T_H2 cells and the IgE responses they promote. Despite the importance of this cytokine, the identity of the cell type that produces the IL-4 needed for the development of T_H2 cells remains controversial. In addition to T_H2 cells themselves, mast cells (*4*), $CD8^+$ T cells (*5*), $\gamma\delta^+$ T cells (*6*), and a subset of $\alpha\beta^+$ T cells expressing NK cell markers (*7*) are all capable of producing IL-4.

NK-like T cells are notable in that they promptly secrete large amounts of IL-4 after in vivo administration of a monoclonal antibody (mAb) to CD3 (*8*). Certain mouse strains, such as SJL and β_2-microglobulin (β_2M)–deficient mice, lack NK-like T cells and do not produce high titers of IL-4 after primary stimulation of their T cell receptors (TCRs) in vivo (*9*, *10*). These animals are also impaired in their ability to produce IgE after immunization with the polyclonal stimulus antibody to IgD (anti-IgD) (*9*, *10*). The correlation between this inability to produce IgE in response to anti-IgD and an absence of IL-4–producing NK-like T cells has led to the suggestion that IL-4 production by NK-like T cells is important for the initiation of T_H2 responses.

Several lines of evidence suggest that NK-like T cells are restricted by the nonpolymorphic major histocompatibility complex (MHC) class I–like molecule CD1. First, $NK1.1^+$ T cells, including those that are $CD4^+$, are easily identified in MHC class II–deficient mice (*11*–*13*), whereas disruption of the gene encoding β_2M, which impairs the expression of CD1, results in the loss of these cells (*13*, *14*). Second, $NK1.1^+$ T cells express a limited repertoire of TCRs comprising an invariant α chain, $V_\alpha14J_\alpha281$, usually paired with a $V_\beta8$, $V_\beta7$, or $V_\beta2$ chain (*15*, *16*), which suggests that they are restricted by a monomorphic ligand. Finally, $NK1.1^+$ T cells can be activated by CD1-expressing cells (*12*, *17*).

To confirm that NK-like T cells require CD1 for their development and to assess the role of CD1-dependent cells in the generation of T_H2 responses, we used gene targeting in embryonic stem (ES) cells to produce CD1-deficient mice. The murine CD1 locus is composed of two closely linked genes, *CD1.1* and *CD1.2*, arranged in opposite transcriptional orientations and spaced approximately 9 kb apart (*18*). We used a gene-targeting construct that deleted almost all of the coding regions of both *CD1.1* and *CD1.2* while maintaining the intergenic sequence (Fig. 1A). Correctly targeted ES cells of strain 129 mice were identified at a frequency of 1 in 75 drug-resistant clones and injected into BALB/c embryos to generate germline chimeras. Southern (DNA) blot analysis confirmed transmission of the targeted allele and deletion of coding sequences from both CD1 genes (Fig. 1B). Homozygous mice were generated at the expected Mendelian frequency and were grossly normal in appearance. To determine whether homozygous mice lacked CD1 expression, thymocytes were analyzed by flow cytometry with the CD1-specific mAb 1B1 (Fig. 1C). CD1 expression was detected on thymocytes from wild-type littermates but was reduced on cells from heterozygous mice and was absent on cells from homozygous mice. Moreover, the CD1-restricted hybridoma DN32.D3 (*16*) could not be activated by thymocytes from homozygous mice (Fig. 1D). Thus, homozygous mice were phenotypically and functionally deficient for CD1 expression.

Several studies have suggested that NK-like T cells may be dependent on CD1 for their maturation (*13*, *14*). In the thymus, NK-like T cells are phenotypically characterized as heat-stable antigen $(HSA)^{-/low}$, $NK1.1^+$, TCR^{int}, $CD44^{high}$, and $CD122^+$ (*19*). In addition, their TCR expression is greatly biased toward $V_\alpha14$ and $V_\beta8$ (*15*, *16*). To determine whether NK-like T cells require CD1 for their development, thymocytes from control and CD1-deficient mice were analyzed by flow cytometry (Fig. 2A). Approximately 10% of the $HSA^{-/low}$ thymocytes from C57BL/6 mice were $V_\beta8^{int}$ $NK1.1^+$, and these cells could also be defined as $V_\beta8^{int}$ $CD44^{high}$ or $V_\beta8^{int}$ $CD122^+$ (*20*) (Fig. 2A). As was consistent with previous observations (*13*, *14*), this population was greatly diminished in β_2M-deficient C57BL/6 mice. When CD1-deficient mice were analyzed for the presence of $HSA^{-/low}$ $V_\beta8^{int}$ $CD44^{high}$ thymocytes (the NK1.1 marker is not expressed in the 129 and BALB/c genetic backgrounds of the CD1-deficient mice), this population was similarly decreased in number (Fig. 2A). Thus, CD1 is the β_2M-dependent molecule required for the development of this thymocyte subset.

Unlike mature peripheral T cells, $HSA^{-/low}$ thymocytes secrete large amounts of both IL-4 and interferon-γ (IFN-γ) after stimulation through their TCRs (*7*, *21*). In

S. T. Smiley and M. H. Kaplan, Department of Cancer Biology, Harvard School of Public Health (HSPH), Boston, MA 02115, USA.
M. J. Grusby, Department of Cancer Biology, HSPH, and Department of Medicine, Harvard Medical School, Boston, MA 02115, USA.

*To whom correspondence should be addressed.